Journal of Hazardous Materials 205–206 (2012) 47–54

Contents lists available at SciVerse ScienceDirect

Journal of Hazardous Materials

journal homepage: www.elsevier.com/locate/jhazmat

Biosorption of the metal-complex dye Acid Black 172 by live and heat-treated biomass of *Pseudomonas* sp. strain DY1: Kinetics and sorption mechanisms

Lin-Na Du[a], Bing Wang[a], Gang Li[b], Sheng Wang[a], David E. Crowley[c,**], Yu-Hua Zhao[a,*]

[a] College of Life Science, Zhejiang University, 310058, Hangzhou, Zhejiang Province, PR China
[b] Department of Agriculture and Biotechnology, Wenzhou Vocational College of Science and Technology, 325006 Wenzhou, Zhejiang Province, PR China
[c] Department of Environmental Science, University of California, Riverside, CA 92521, United States

ARTICLE INFO

Article history:
Received 4 August 2011
Received in revised form 3 November 2011
Accepted 1 December 2011
Available online 8 December 2011

Keywords:
Biosorption
Pseudomonas sp.
Metal-complex dye
FTIR
AFM

ABSTRACT

The ability of *Pseudomonas* sp. strain DY1 to adsorb Acid Black 172 was studied to determine the kinetics and mechanisms involved in biosorption of the dye. Kinetic data for adsorption fit a pseudo-second-order model. Increased initial dye concentration could significantly enhance the amount of dye adsorbed by heat-treated biomass in which the maximum amount of dye adsorbed was as high as 2.98 mmol/g biomass, whereas it had no significant influence on dye sorption by live biomass. As treated temperature increased, the biomass showed gradual increase of dye sorption ability. Experiments using potentiometric titration and Fourier transform infrared spectroscopy (FTIR) indicated that amine groups (NH_2) played a prominent role in biosorption of Acid Black 172. Scanning electron microscopy (SEM), atomic force microscopy (AFM) and transmission electron microscopy (TEM) analysis indicated that heat treatment of the biomass increased the permeability of the cell walls and denatured the intracellular proteins. The results of biosorption experiments by different cell components confirmed that intracellular proteins contributed to the increased biosorption of Acid Black 172 by heat-treated biomass. The data suggest that biomass produced by this strain may have application for removal of metal-complex dyes from wastewater streams generated from the dye products industry.

1. Introduction

Biosorption is an attractive method for removal of toxic synthetic dyes from wastewater streams that are generated by the textile and dye product industries [1,2]. Many synthetic dyes are both toxic and carcinogenic and are not easily degraded to safe concentrations in the environment [3,4]. A variety of low-cost biosorbents including biomass produced from bacteria, fungi, algae, yeast and other materials have been used to remove dyes from wastewater [5–16], but vary in their performance to adsorb different types of dyes. Among these researches, there is very little information on the biosorption of metal-complex dyes, although the metals contained in metal-complex dyes such as chromium, cobalt and copper, are also hazardous to the environment [16].

One method for improving the efficiency of biosorbents is through modification of biomass using various chemical agents, or by oven heating or autoclaving, or by genetic modification of the cells to change their sorption properties [2]. In many cases, sorption by dead cells has been found to be much greater than with live cells, although the reason for this phenomenon is not clear. Hu observed that removal of selected dyes by dead cells of *Aeromonas* sp. was more efficient than that which could be achieved using live cells, and suggested that the increased biosorption was due to a larger surface area of the dried biomass [17]. Likewise, heat treatment of biomass from *Trametes versicolor* results in better sorption of the benzidine based textile dyes "Direct Blue 1 and Direct Red 128" [8], and dead biomass of *Bacillus sphaericus* has been shown to be more effective for adsorbing heavy metals than live biomass, although neither of these studies proposed an explanation as to why dead biomass would be more effective [18]. In addition, various functional groups on the fungal biosorbents including carboxyl, amino and phosphate groups have been shown to play an important role in biosorption of various dyes [2,13], while only limited information is available on the biosorption sites of bacterial biosorbents.

Pseudomonas sp. strains have been widely used as a kind of biosorbent and can be attained free or at a very low cost [2]. In previous research, we have shown that *Pseudomonas* sp. strain DY1 is an efficient sorbent for Acid Black 172 [19]. The present study was aimed at investigating differences in the biosorption of the metal-complex dye of Acid Black 172 by the live and heat-treated biomass of strain DY1, and to characterize the mechanisms involved in increased sorption following heat-treatment of the biomass.

* Corresponding author. Tel.: +86 571 88208557.
** Corresponding author. Tel.: +1 951 827 3785.
E-mail addresses: crowley@ucr.edu (D.E. Crowley), yhzhao225@zju.edu.cn (Y.-H. Zhao).

0304-3894/$ – see front matter © 2011 Elsevier B.V. All rights reserved.
doi:10.1016/j.jhazmat.2011.12.001

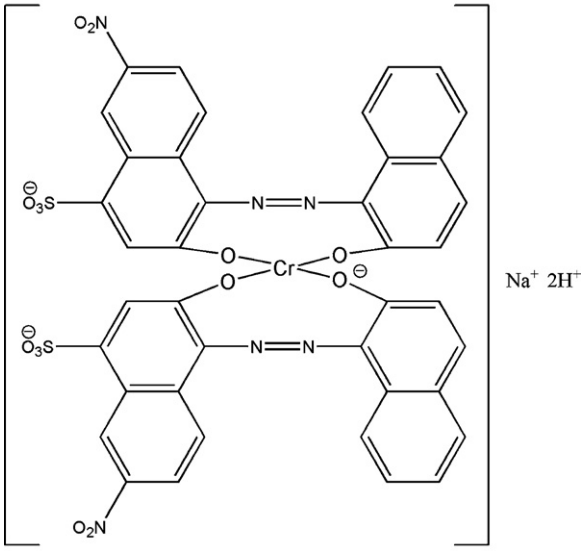

Fig. 1. Chemical structure of Acid Black 172.

2. Materials and methods

2.1. Preparation of dye solution and biomass

Dye solutions were prepared by dissolving Acid Black 172 (Fig. 1) into distilled water at a final concentration of 100 mg/L. *Pseudomonas* sp. strain DY1 was cultured in LB medium (200 mL) in 500 mL flask shaken at 200 rpm, at 30 °C for 12 h. All cultures were centrifuged at 8000 rpm for 10 min and washed three times with distilled water to collect the live biomass. Heat-treated biomass was acquired by heating the cells at 100 °C for 30 min.

2.2. Adsorption experiments by live and heat-treated biomass

Adsorption experiments were carried out by adding a fixed amount of adsorbent (0.05 g dry weight) to the replicate flasks containing 100 mL of the dye solution. The dye solutions were adjusted to pH values ranging from pH 3.0 to pH 9.0, after which live or heat-treated biomass was added to the flasks to measure the equilibrium concentrations of dye at 1 pH unit increments. At several intervals, 3 mL aliquots of dye solution was taken from the flasks and analyzed using the UV-3100PC spectrophotometer (Shanghai MAPADA Instruments Co., Ltd.). The mixture was then centrifuged at 10,000 rpm for 10 min, and the supernatant was analyzed at λ_{max} (572 nm) of Acid Black 172. The biosorption percentage was calculated by the following formula:

$$\text{Biosorption percentage } (\%) = \frac{A_i - A_f}{A_i} \times 100$$

A_i is the initial absorbance; A_f is the final absorbance.

In order to determine the effect of initial dye concentration on biosorption, the live or heat-treated biomass (0.05 g dry weight) was added to the flasks containing 100 mL dye solution (100–1000 mg/L), respectively. After 1 h incubation, 4 mL samples were collected and used to determine the dye sorption.

To determine the effect of different treated temperatures on the dye sorption ability of the cells, different treated temperatures ranged from 4 °C to 100 °C were employed to treat the live cells, and then used to adsorb 100 mg/L dye solution.

2.3. Determination of surface functional groups

The surface functional groups of live and heat-treated biomass of strain DY1 were determined by the potentiometric titration and Fourier transform infrared spectroscopy (FTIR) methods.

For the potentiometric titration studies, samples of the live and heat-treated biomass were suspended separately in 100 mL double-distilled water containing 0.1 M NaCl. During the titration experiments, N_2 was continuously sparged into the bacterial suspension to obtain oxygen-free conditions. The suspension was titrated using 0.1 M NaOH and 0.1 M HCl. A predetermined amount of HCl was added to adjust the pH to 4.0. After equilibration for 1 h, the suspension was titrated slowly with NaOH to pH 10.0 with 20 min equilibration time.

For FTIR measurements, the live and heat-treated biomass was lyophilized in a freeze dryer. A Bruker Veefor 22 FTIR spectrometer was used to collect FTIR spectra over the range from 400 to 4000 cm^{-1}.

2.4. Determination of surface characteristics

Scanning electron microscopy (SEM) and atomic force microscopy (AFM) were used to study the surface characteristics of strain DY1. To prepare specimens for SEM, live and heat-treated biomass was fixed with 2.5% glutaraldehyde at 4 °C overnight, then washed separately with 1% osmium and phosphate buffer 3 times, and dehydrated using a gradient series with ethanol. The dehydrated samples were dried and sputter-coated with gold, and observed on the SEM.

For AFM analysis, aliquots of live and heat-treated biomass (before and after dye sorption) were distributed uniformly in sterile distilled water, mounted on a mica sheet, and air dried at room temperature (22–28 °C). The specimens were viewed using a multimode SPM NanoScope 3D Atomic force microscope (Veeco Ltd., USA). Imaging was carried out using monocrystalline silicon tips in tapping mode.

2.5. Determination of structural characteristics

The structural characteristics of live and heat-treated biomass of strain DY1 were analyzed by transmission electron microscopy (TEM). For preparation of the TEM samples, aliquots of live and heat-treated biomass of strain DY1 were immobilized in agarose at 4 °C overnight. The samples were washed with phosphate buffer (pH 7.0) 3 times, and dehydrated in alcohol. The dehydrated samples were then immobilized and cut into 70–90 nm shin sheets, and observed by TEM (JEM-1230, JEOL).

2.6. Biosorption experiments by different cell components

Samples of live and heat-treated biomass were ultrasonicated and centrifuged at 12,000 rpm for 15 min. The products from the ultrasonication were then treated as follows: (1) the sediments containing cell debris after ultrasonication of the live biomass were divided into two equal parts, one part was used to adsorb 100 mg/L Acid Black 172; the other part was heated at 100 °C for 30 min and then used to adsorb the dye; (2) the soluble intracellular proteins in the supernatants were precipitated with ammonium sulfate and collected by centrifugation; after which the proteins were heated at 100 °C for 30 min and then used to adsorb the dye.

To further explore the role of intracellular proteins in dye biosorption by the heat-treated biomass, FTIR measurements were carried out on the dye-free and dye-loaded proteins. The samples were lyophilized in a freeze dryer, and a Bruker Veefor 22 FTIR spectrometer was used to collect FTIR spectra over the range from 400 to 4000 cm^{-1}.

Table 1
The biosorption rate constants (k) and the q_e values from the pseudo-second-order kinetics for biosorption of Acid Black 172 by live or heat-treated biomass of strain DY1.

Adsorbent	pH	Pseudo-second-order kinetic model		
		k (g/mg min)	q_e (mg/g)	R^2
Live biomass	3.0	0.0002	759.3	0.9699
	4.0	0.0051	42.6	0.9800
	5.0	0.1328	22.1	0.9217
	6.0	0.0074	23.3	0.8543
	7.0	0.0109	22.2	0.8251
	8.0	0.0020	27.9	0.8370
	9.0	0.0407	21.3	0.8689
Heat-treated biomass	3.0	0.0035	1811.6	0.9999
	4.0	0.0006	1658.4	0.9998
	5.0	0.0002	1280.4	0.9967
	6.0	0.0002	1158.7	0.9960
	7.0	0.0002	1102.5	0.9949
	8.0	0.0002	1071.8	0.9958
	9.0	0.0002	1073.0	0.9955

3. Results and discussion

3.1. Analysis of batch biosorption experiments

3.1.1. Biosorption kinetics by live and heat-treated biomass at different pHs

The adsorption of Acid Black 172 by live and heat-treated biomass of strain DY1 was modeled using Lagergren pseudo-first-order and pseudo-second-order kinetic models. However, the data did not fit the Lagergren pseudo-first-order model well (data not shown). Therefore, the pseudo-second-order kinetics as shown in the following the equation was employed to describe the kinetic behavior in the dye biosorption process [1,2]:

$$\frac{dq_t}{dt} = k(q_e - q_t)^2 \quad (1)$$

where q_t is the amount of dye adsorbed by the adsorbent at time t (mg/g biomass), q_e is the amount of dye adsorbed at equilibrium (mg/g biomass), k is the pseudo-second order rate constant (g/mg min).

The integration of Eq. (1) with the boundary conditions leads to:

$$q_t = \frac{kq_e^2 t}{1 + kq_e t} \quad (2)$$

Eq. (2) also can be written as:

$$\frac{t}{q_t} = \frac{t}{q_e} + \frac{1}{kq_e^2} \quad (3)$$

In Eq. (3), the relationship between t/q_t and t is linear. Therefore, the data were transformed to fit the equation and a curve was constructed by linear regression (Table 1). Compared to the results obtained for biosorption by live biomass, the experimental data for the heat-treated biomass fit the pseudo-second-order model better, with corresponding correlation coefficients all more than 0.99. Moreover, the amount of dye adsorbed at equilibrium decreased as the pH value increased, and the maximum amount of dye adsorbed at equilibrium by heat-treated biomass was 1811.2 mg/g biomass, while it was only 759.3 mg/g biomass by live biomass (Table 1).

3.1.2. Effect of initial dye concentration and different treated temperatures on biosorption

The effect of initial dye concentration on biosorption by the live and heat-treated biomass is presented in Fig. 2. It is clear that the amount of dye adsorbed by heat-treated biomass increased with the initial dye concentration, and the maximum amount of the dye adsorbed could reach to 2.98 mmol/g biomass. However, the dye amount adsorbed by the live biomass had no significant change as the initial dye concentration increased. Moreover, Fig. 2 also showed that different treated temperature could significantly affect the dye sorption ability of the cells. There was no significant difference between dye sorption by the cells treated with 4 °C and 30 °C, while the dye sorption increased significantly as the treated temperature increased from 30 °C to 100 °C.

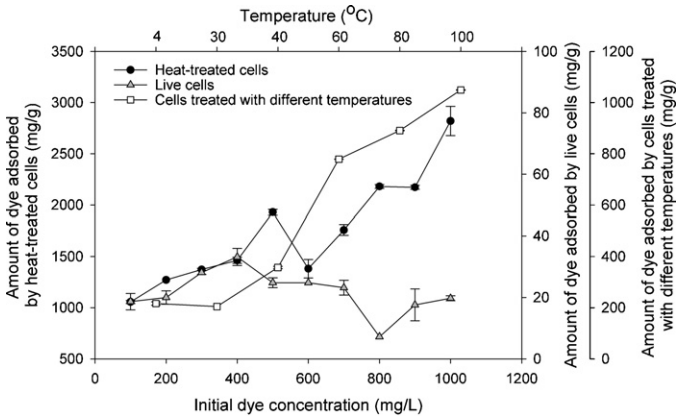

Fig. 2. Effect of initial dye concentration and different treated temperatures on biosorption by live and heat-treated biomass.

We compared the values obtained for biosorption of Acid Black 172 in this research with those obtained in prior researches on synthetic dyes. Akar et al. investigated dye biosorption by untreated olive pomace, and reported the maximum amount of the dye adsorbed was 0.108 mmol/g biomass [20]; Akar et al. also investigated dye biosorption using a mixed biosorbent of macro-fungus *Agaricus bisporus* and *Thuja orientalis* cones, in which case the maximum amount of dye adsorbed was 0.185 mmol/g biomass at 45 °C [13]. Vijayaraghavan et al. studied the biosorption of methylene blue from aqueous solution using free and polysulfone-immobilized *Corynebacterium glutamicum*, whereby the maximum amount of adsorbed dye was about 0.33 mmol/g biomass [21]. In the research reported here, heat-treated biomass of strain DY1 could adsorb Acid Black 172 (1000 mg/L) at concentrations up to 2.98 mmol/g biomass, indicating that the heat-treated biomass of strain DY1 was an efficient adsorbent. The observation that heat-treated biomass had a better adsorptive capacity than live biomass prompted further experiments to determine the mechanism for improved sorption following the heat-treatment.

3.2. Surface functional groups of live and heat-treated biomass and possible mechanism of the biosorption

Potentiometric titrations can determine the acid dissociation constants (pK_a) and concentrations of different proton binding sites on bacterial cell walls [22]. The titration curves and pK_a spectra of both live and heat-treated biomass are depicted in Fig. 3. A linear programming method was applied to calculate the concentrations of different functional groups distributed on cell surface. All possible proton binding sites were determined according to Cox et al. [23]. The groups with pK_a 4.0 were most probably carboxyl groups. Groups with pK_a 6.1 and 6.4 of live biomass and groups with pK_a 6.2 and 7.4 of heat-treated biomass were most likely phosphoryl groups. The groups with pK_a 8.2, 8.5 and 10.0 of live biomass and groups with pK_a 8.6, 8.8 and 10.0 of heat-treated biomass were considered to be amine groups and hydroxyl groups (Fig. 3). Comparing the pK_a spectra of both samples, the concentrations of the functional amine groups which were hypothesized to contribute to the biosorption of the dye were greater in the heat-treated biomass.

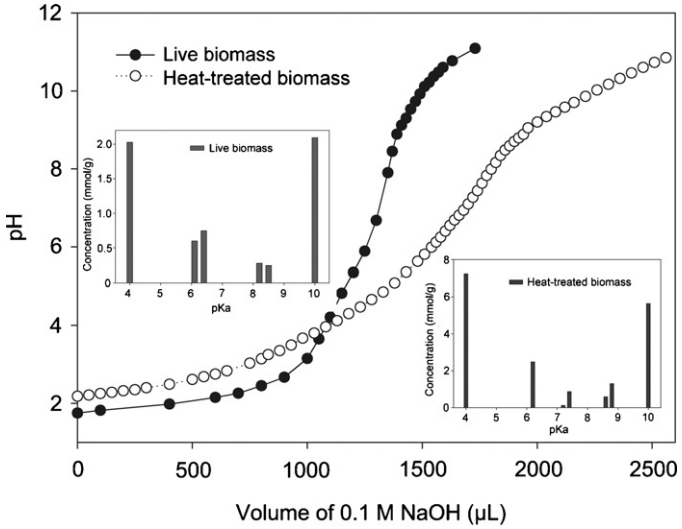

Fig. 3. Potentiometric titrations of live and heat-treated biomass. The inset figures are the pK_a spectra for live and heat-treated biomass.

FTIR spectra also can reveal the surface functional groups on the surface of the biomass [24]. The FTIR spectra of dye-loaded and dye-free live and heat-treated biomass of strain DY1 are shown in Fig. 4. The possible assignments of the absorption bands are summarized in Table 2 according to previous studies [25–27]. The spectrum of the dye-free live biomass showed a broad and strong peak at 3304 cm^{-1}, which is attributed to the NH_2 stretching vibrations in polysaccharides and proteins. In the spectrum of dye-loaded live biomass, this peak was shifted to the 3321 cm^{-1} region and significantly decreased compared to that of the dye-free live biomass, indicating the binding of the dye with NH_2 groups. There was no shift in the peak (3292 cm^{-1}) position in the spectrum of the dye-loaded and dye-free heat-treated biomass, while the intensity of this peak in the spectrum of dye-loaded heat-treated biomass decreased compared to that of dye-free heat-treated biomass. This significant change in the intensity of peak at 3292 cm^{-1} indicated the binding of the dye with NH_2 groups. The spectrum of the dye-free live biomass showed two strong peaks at 1653 cm^{-1} and 1539 cm^{-1} region due to the presence of amine groups (NH_2), or carbonyl (C═O) or C═N stretching (amide I and II). In the spectrum of dye-loaded live biomass, these peaks were shifted to 1655 cm^{-1} and 1533 cm^{-1} region, and the peak at

Table 2
FTIR identification of live and heat-treated biomass of strain DY1.

Possible assignments	Wave number (cm^{-1})
H-bonded OH groups (polysaccharides)	3783
NH_2 stretching (proteins)	3300
Aliphatic C-H stretching (fatty acids)	2960–2850
NH_2 bending, C═O, C═N stretching (amide I and II)	1660–1535
C—H deformations of CH_2 or CH_3 groups in aliphatics	1467–1455
C—H bending, —CH_3 stretch, COO—symmetric stretch (amino acid side chains, fatty acids)	1396–1389
C—N stretching (amide III), PO_2^- asymmetric stretching (mainly nucleic acids with the little contribution from phospholipids)	1240–1235
$CONR_2$ bonding, CO—O—C asymmetric stretching (glycogen and nucleic acids)	1200–1150
CH_2OH, C—O, P—O_2 stretching (glycopeptides, ribose)	1150–1000
P—O—C, P—O—P stretching (phospholipids, ribose phosphate chain pyrophosphate)	965–760
C—O—C, P—O—C bonding (RNA, aromatics)	650–485

Assignments according to the references [25–27].

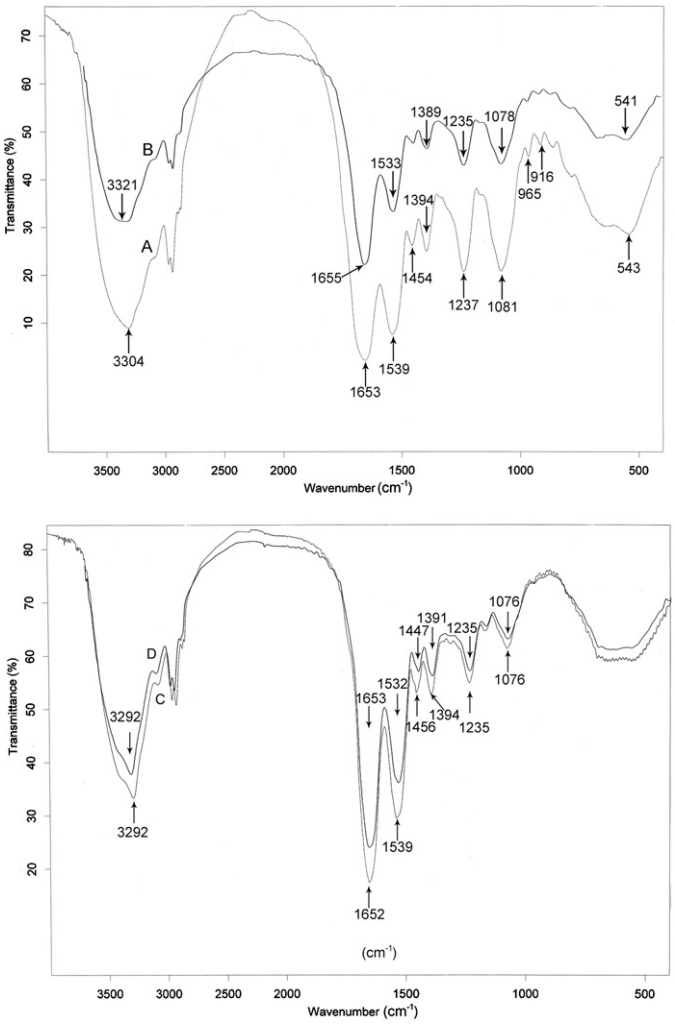

Fig. 4. FTIR spectra for (A) the live biomass of strain DY1; (B) the live biomass of strain DY1 with dye sorption; (C) the heat-treated biomass of strain DY1; (D) the heat-treated biomass of strain DY1 with dye sorption.

1533 cm^{-1} region decreased significantly compared to that of the dye-free live biomass, indicating the strong interaction of the dye with amide I and II functional groups. In the spectrum of dye-loaded heat-treated biomass, the peak at 1652 cm^{-1} had no significant shift, while the peak at 1539 cm^{-1} region was shifted to 1532 cm^{-1} region, and the peak at 1532 cm^{-1} region also decreased compared to that of the dye-free heat-treated biomass. This further ascertained the strong interaction of the dye with amide I and II groups. The peak at 1396–1389 cm^{-1} was mainly due to the C—H bending, —CH_3 stretch, or COO—symmetric stretch. The peak at 1240–1235 cm^{-1} was attributed to the C—N stretching (amide III) and PO_2^- asymmetric stretching (mainly nucleic acids with the little contribution from phospholipids). The intensity of these peaks in the dye-loaded live biomass also decreased significantly compared to that of the dye-free live biomass, while it decreased slightly in the dye-loaded heat-treated biomass compared to that of dye-free heat-treated biomass. The peak at 1200–1150 cm^{-1} was due to the $CONR_2$ and CO—O—C asymmetric stretching (mainly from glycogen and nucleic acids). This peak in the spectrum of the live biomass was smaller than that of heat-treated biomass. The peak at 1150–1000 cm^{-1} was attributed to the CH_2OH, C—O or P—O_2 stretching coming from glycopeptides or ribose. The intensity of this peak in the spectrum of dye-loaded live biomass decreased compared to that of dye-free live biomass, while there was no

significant change in the spectrum of the dye-free and dye-loaded heat-treated biomass. The overall spectral analysis strongly supported the hypothesis that the NH_2 groups played a major role in the biosorption of Acid Black 172 by the strain. The NH_2 groups of the biomass will be protonated at pH lower than its pK_a value of 9.14 [28].

$$\text{Biomass} - NH_2 + H^+ \overset{pH<9.14}{\rightleftarrows} \text{Biomass} - NH_3{}^+$$

In the aqueous solution, Acid Black 172 is dissociated and converted into Na^+/H^+ and anionic dye ions at pH larger than pK_a value (−1.34) of sulfonic groups [29].

$$\text{Dye} - ONa \overset{H_2O}{\rightleftarrows} \text{Dye} - O^- + Na^+$$

$$\text{Dye} - (SO_3H)_2 \underset{pH>-1.34}{\overset{H_2O}{\rightleftarrows}} \text{Dye} - (SO_3{}^-)_2 + 2H^+$$

Therefore, the possible binding mechanism of the dye at pH larger than −1.34 and lower than 9.14 could be proposed as follows, which could be explained on the basis of the electrostatic interaction between the negative groups of the dye and the positive groups of the biomass:

$$\text{Biomass} - NH_3{}^+ + \text{Dye} - O^- \overset{-1.34<pH<9.14}{\rightleftarrows} \text{Biomass} - NH_3{}^+ \cdots {}^-O - \text{Dye}$$

$$\text{Biomass} - NH_3{}^+ + \text{Dye} - SO_3{}^- \overset{-1.34<pH<9.14}{\rightleftarrows} \text{Biomass} - NH_3{}^+ \cdots {}^-O_3S - \text{Dye}$$

However, the binding mechanism could not explained via electrostatic interaction at pH > 9.14, because NH_2 groups of the biomass exist as neutral form (Biomass–NH_2) at pH larger than its pK_a value. Therefore, other binding mechanisms, e.g. hydrogen bonding, might involved in the dye sorption at pH > 9.14.

Observed differences in peak position and intensity in the spectra of dye-free and dye-loaded live biomass indicate that the functional groups in the surface of live biomass played an important role in biosorption of the dye. It was noticed that the amount of the P—O—C and P—O—P stretching coming from the phospholipids or ribose phosphate chain pyrophosphate (peaks at 965–760 cm^{-1}) on the surface of the heat-treated biomass was significantly lower than that of the live biomass, suggesting that the cell wall structure was no longer intact following heat treatment. Therefore, we speculated that the permeability of the cell walls of heat-treated cells was greater than that of live cells, and that the dye could enter into the interior of the heat-treated cells leading to an increase in biosorption.

3.3. Cellular morphology characteristics of the live and heat-treated biomass

To directly determine the characteristics of cellular morphology, SEM, AFM and TEM analyses were conducted on both the live and heat-treated biomass. The SEM images of live and heat-treated cells are presented in Fig. 5. It was observed that the surfaces of the live cells were smooth, while the surfaces of the heat-treated cells were porous and covered by tiny particles (Fig. 5). These tiny particles might be the cell contents that were released during the process of heating, suggesting that the permeability of cell walls of the heat-treated cells was enhanced. The pores in the surface of the heat-treated cells also indicated the high permeability of the cell wall.

AFM is an ideal tool to determine the cellular morphology. The AFM images of biomass produced by strain DY1 are shown in Fig. 6 and line analyses of these images are presented in Table 3. As seen in Fig. 6, the cell walls of live cells with (A) and without (B) dye were smooth and intact, while the heat-treated cells with (D) and without (C) dye showed rough, porous and ruptured cell walls, which implied that the permeability of the cell wall of heat-treated cells was greater than that of live cells. Results of topography analysis of the live biomass before and after dye sorption in Table 3 showed that there was no significant variation in cell size ($P > 0.05$), whereas there was a significant increase in the arithmetic average roughness (R_a, $P < 0.05$) and root mean square roughness (RMS, $P < 0.05$) after dye sorption compared to that before dye sorption. Wang et al. have reported a surface roughness increase following metallization of nickel by *E. coli* [30]. Kazy et al. have also reported a similar variation in the surface roughness of *Pseudomonas* cells following uranium and thorium sorption [31]. A possible reason for the increased surface roughness after dye sorption, supported by the previous studies, might be that the dye interactions with functional groups on the surface of cells changed the surface architecture. There was no significant variation ($P > 0.05$) in both cell size and surface roughness of the heat-treated biomass before and after dye sorption (Table 3), suggesting that the cell wall contributed little in the increased dye sorption by heat-treated biomass. Compared to the live biomass, there was a significant increase in the R_a ($P < 0.001$) and RMS ($P < 0.001$) of the heat-treated biomass, whereas there was no significant variation in the cell size, which indicated that the increase dye sorption by heat-treated biomass was not due to increased surface area (Table 3). Besides, the increased R_a and RMS values of heat-treated cells also indicated that the bacterial cells had been destroyed after heating which further increased the permeability of the cell walls.

Table 3
Bacterial cell dimensions and surface roughness of live and heat-treated biomass (before and after dye sorption).

	Length (μm)	Width (μm)	Height (nm)	Roughness (nm)	
				R_a	RMS
A	2.09 ± 0.07	1.02 ± 0.07	186.1 ± 13.7	34.8 ± 3.3	50.1 ± 3.9
B	2.40 ± 0.14	1.07 ± 0.08	175.3 ± 14.9	51.3 ± 4.8	69.3 ± 5.1
C	2.50 ± 0.22	1.16 ± 0.08	357.3 ± 11.7	86.7 ± 5.8	112.3 ± 4.2
D	2.34 ± 0.12	1.23 ± 0.05	330.7 ± 19.9	90.2 ± 6.4	118.0 ± 6.6

Ra: arithmetic average roughness; RMS: root mean square roughness; A: live biomass; B: live biomass with dye; C: heat-treated biomass; D: heat-treated biomass with dye. Cell dimensions were determined from topography analysis of AFM images.

The structural status of the live and heat-treated cells detected by TEM is presented in Fig. 7. Structurally, the differences between the live and heat-treated cells were significant. The contents of the heat-treated cells were congregated and distributed unevenly closely to the cell wall, while the contents of the live cells were uniformly distributed in the cells. The cell walls of the live cells seemed to be tighter than that of the heat-treated cells. It was clear that several parts of the cell walls of the heat-treated cells were looser and thinner, suggesting that the heat-treated cells would have greater permeability. Besides, the bead-like part of the heat-treated cells in Fig. 7 might be comprised of cell contents that released during the heating process, also suggesting that the permeability of the cell walls of the heat-treated cells was greater than that of the live cells. Therefore, we supposed that the increased biosorption of dye by the heat-treated biomass was due to the greater permeability of the cell wall, so that the dye macromolecule could enter into the cells and be adsorbed to the possible adsorption sites in the interior of the cells.

3.4. Intracellular proteins played a major role in the increased biosorption by the heat-treated biomass

To better understand the different dye sorption by the live and heat-treated biomass, dye sorption was studied for the different cell components (Fig. 8). Results indicated that dye sorption by sediments produced from ultrasonication of the live biomass were not significantly different from the intact live cell biomass ($P > 0.05$),

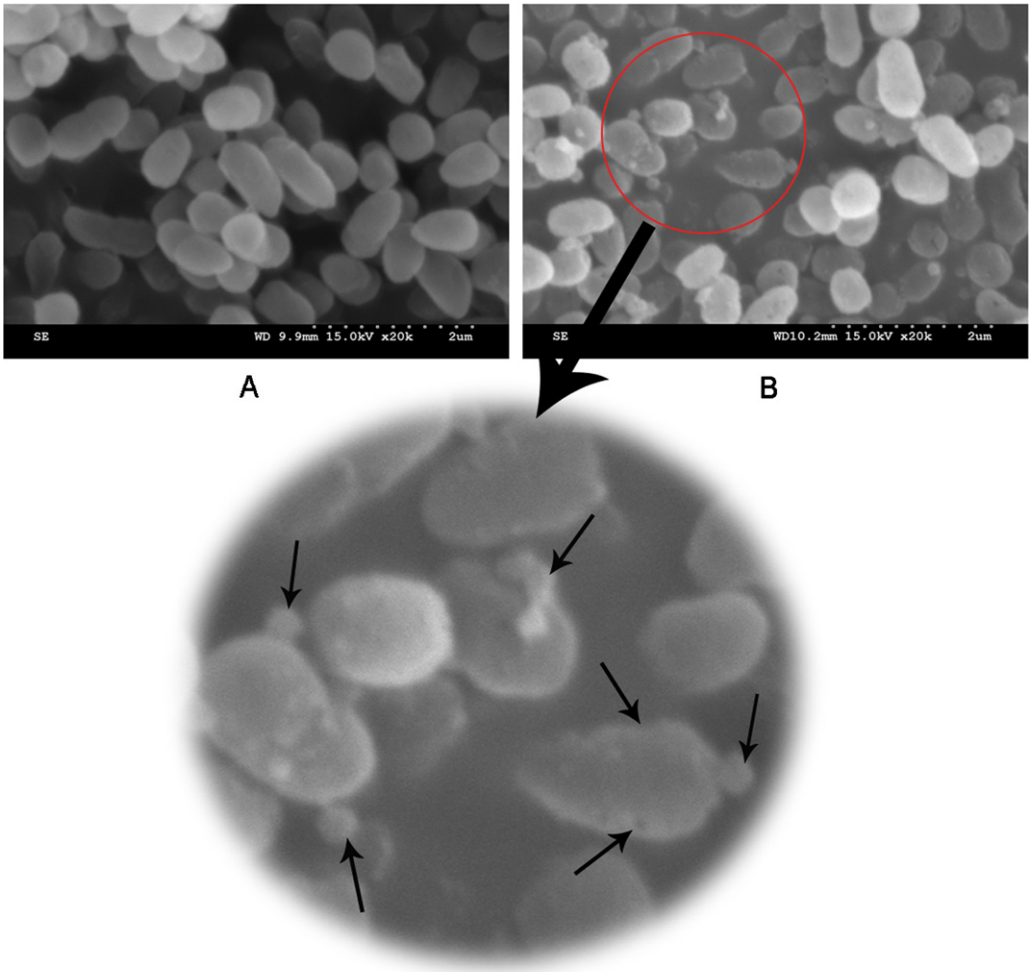

Fig. 5. SEM images of (A) the live biomass of strain DY1; (B) the heat-treated biomass of strain DY1. The enlarged part is the SEM images of the heat-treated biomass, in which the parts pointed with the arrow are the pores and tiny particles on the surface of heat-treated cells.

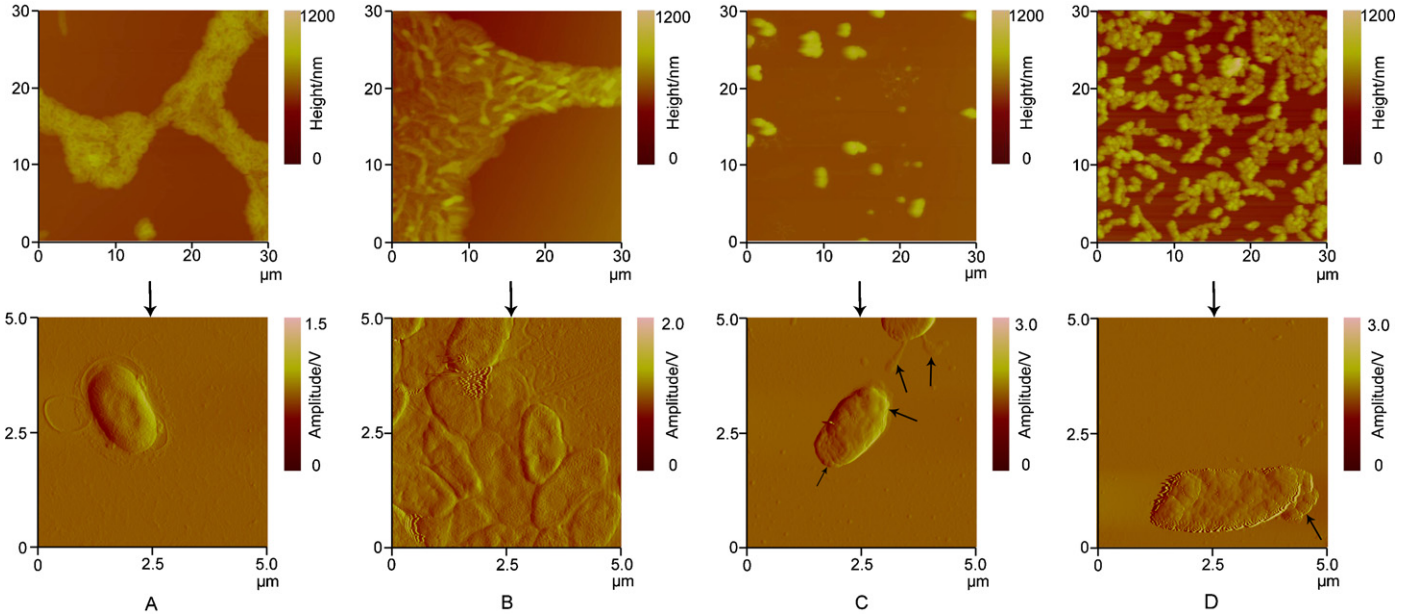

Fig. 6. AFM images of the live biomass of strain DY1 with (B) and without (A) dye; the heat-treated biomass of strain DY1 with (D) and without (C) dye. The parts pointed with the arrow in images (C) and (D) are the porous and ruptured parts on the surface of heat-treated cells.

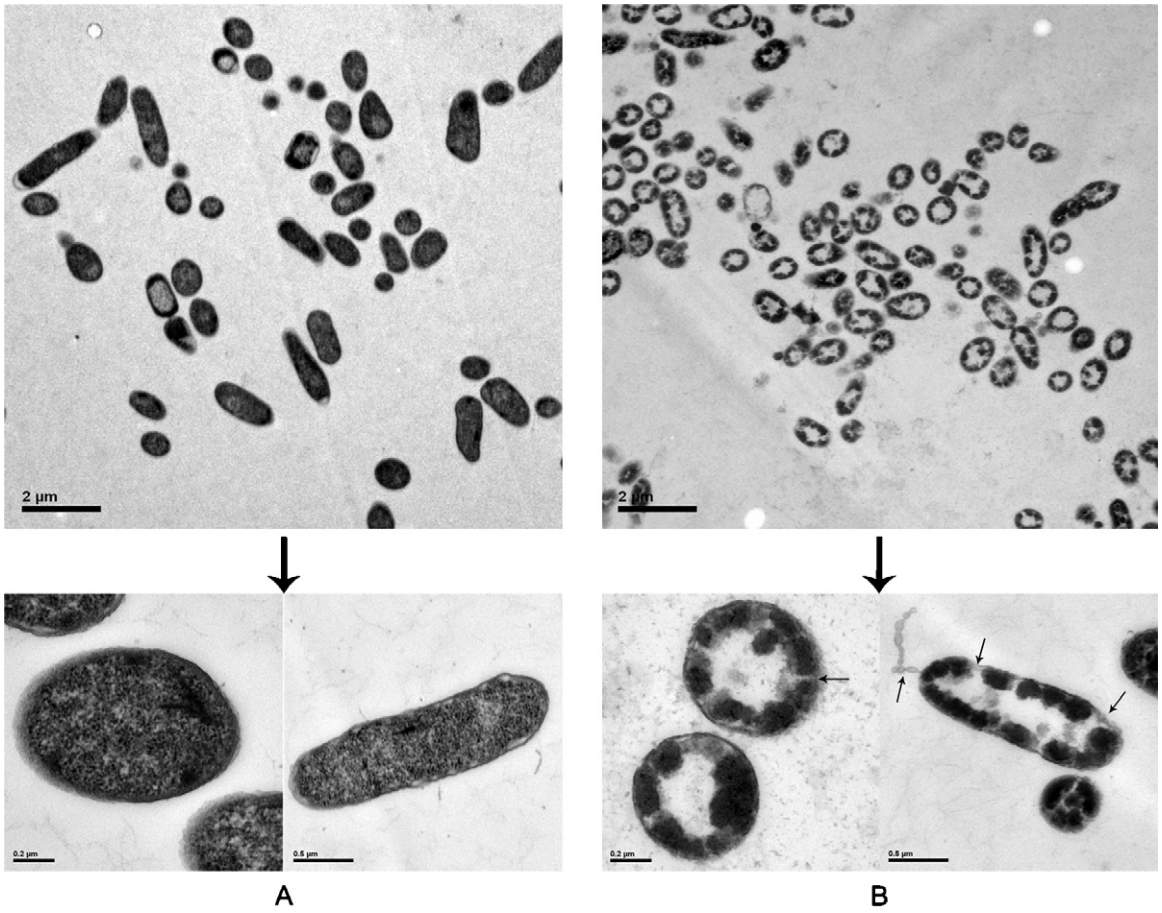

Fig. 7. TEM images of (A) the live biomass of strain DY1; (B) the heat-treated biomass of strain DY1. The pores and tiny particles on the surface of heat-treated cells are pointed with the arrow.

suggesting that the cell wall played a major role in biosorption of Acid Black 172 since most of the sediments after ultrasonication were cell wall fragments. Under the reaction conditions, 29.8% sorption occurred with cell wall fragments after heating, which was about just 20% greater than that measured for cell wall fragments without heating ($P < 0.05$). However, the dye sorption by the heat-treated biomass could reach to 80%, which was about 70% increase compared to the cell wall fragments without heating ($P < 0.05$). Therefore, the cell wall contributed little to the increased biosorption by heat-treated biomass. Besides, the sorption of dye by the intracellular proteins was about 93.2%, indicating that the denaturalized proteins played a prominent role in the increased biosorption by the heat-treated biomass.

To better evaluate the possible role of intracellular proteins in the increased dye sorption by heat-treated biomass, FTIR analysis was carried out on the dye-free and dye-loaded intracellular proteins (Fig. 9). The spectrum of dye-loaded proteins showed a strong peak at 3445 cm^{-1}, which was due to the stretching of —OH

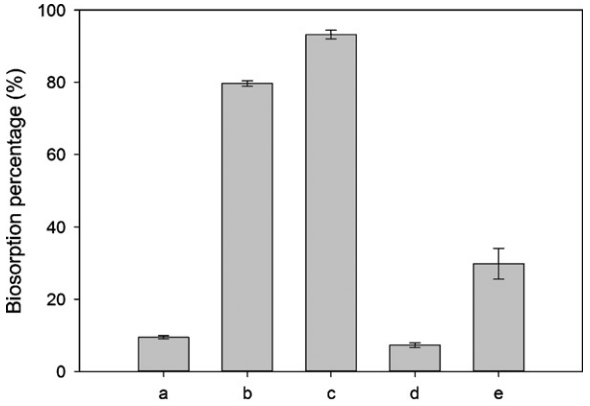

Fig. 8. Biosorption of Acid Black 172 by different cell components. (a) Live biomass; (b) heat-treated biomass; (c) intracellular proteins after heating; (d) the cell wall fragments without heating; (e) the cell wall fragments after heating.

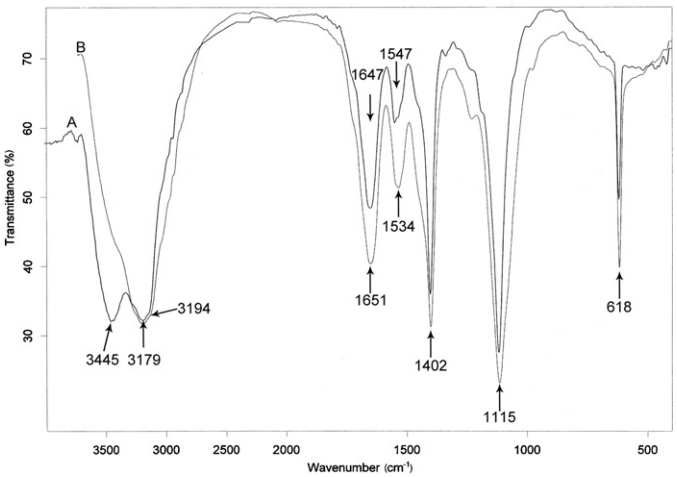

Fig. 9. FTIR spectra for the intracellular proteins with (A) and without (B) dye sorption.

(H_2O interference). Compared to the dye-loaded proteins, the peak at 3194 cm^{-1} (—NH or —OH stretching) of the dye-free proteins was significantly shifted to 3179 cm^{-1} after dye sorption, while the intensity had no significant change. The peaks at 1651 cm^{-1} and 1534 cm^{-1} of dye-free proteins were attributed to the stretching of amine groups that shifted to 1647 cm^{-1} and 1547 cm^{-1} after dye sorption, respectively, and the intensity also decreased significantly, indicating the interaction of dye with amine groups. The peaks at 1401 cm^{-1} (—CHO or —COO stretching), 1115 cm^{-1} (—CO or —S═O stretching), and 619 cm^{-1} (—C—Cl stretching) had no significant change after dye sorption, which indicated that these groups were not responsible for the dye sorption by the intracellular proteins. Therefore, the latent dye sorption sites in intracellular proteins exist in the form of amine groups.

Previous studies observed that most of dead microorganisms showed higher sorption ability than live microorganisms, while the reasons remain unclear [32,33]. Based on the present work, we propose that the increase biosorption of dye by the heat-treated biomass compared to that by live biomass could be due to increased permeability of the cell wall after heating, such that the dye could enter into the cells and be adsorbed to the intracellular adsorption sites (amine groups) in the form of intracellular proteins.

4. Conclusions

Heat-treated biomass of *Pseudomonas* sp. strain DY1 was observed to adsorb Acid Black 172 more efficiently than live biomass. The maximum amount of the dye adsorbed by the heat-treated biomass could reach to 2.98 mmol/g biomass. Amine groups played a major role in the biosorption of Acid Black 172. Moreover, heating of the biomass significantly increased the permeability of the cell wall so that the dye could enter into the cells and be adsorbed to intracellular proteins. The availability of inexpensive biosorbents such as bacterial biomass provides an economically feasible method for removal of dyes which can be optimized by heating the biomass prior to use as a sorbent. The long term fate of dyes following adsorption to biomass remains an open question; therefore, further tests should focus on the fate of the metal-complex dyes following removal from wastewater.

Acknowledgments

This study was supported by the National Hi-Tech Research and Development Program (863) of China (no. 2007AA06Z329, http://program.most.gov.cn), the Science and Technology Project of Zhejiang Province (2008C13014-3, http://www.zjkjt.gov.cn), the National Natural Science Foundation of China (31070079, http://www.nsfc.gov.cn), and the International Cooperation Project in Science and Technology of Zhejiang Province (nos. 2008C14038, 2011C13016, http://www.zjkjt.gov.cn). The funders had no role in study design, data collection and analysis, decision to publish, or preparation of the manuscript. The authors are grateful to the engineer Min Liu for AFM analysis.

References

[1] Z. Aksu, Application of biosorption for the removal of organic pollutants: a review, Process Biochem. 40 (2005) 997–1026.
[2] K. Vijayaraghavan, Y.S. Yun, Bacterial biosorbents and biosorption, Biotechnol. Adv. 26 (2008) 266–291.
[3] E. Forgacs, T. Cserháti, G. Oros, Removal of synthetic dyes from wastewaters: a review, Environ. Int. 30 (2004) 953–971.
[4] F.P. Van der Zee, S. Villaverde, Combined anaerobic–aerobic treatment of azo dyes—a short review of bioreactor studies, Water Res. 39 (2005) 1425–1440.
[5] Z. Aksu, G. Dönmez, A comparative study on the biosorption characteristics some yeasts for Remazol Blue reactive dye, Chemosphere 50 (2003) 1075–1083.
[6] T.V.N. Padmesh, K. Vijayaraghavan, G. Sekaran, M. Velan, Batch and column studies on biosorption of acid dyes on fresh water macro alga *Azolla filiculoides*, J. Hazard. Mater. B125 (2005) 121–129.
[7] G. Bayramoğlu, G. Çelik, M.Y. Arica, Biosorption of Reactive Blue 4 dye by native and treated fungus *Phanerocheate chrysosporium*: batch and continuous flow system studies, J. Hazard. Mater. B137 (2006) 1689–1697.
[8] G. Bayramoğlu, M.Y. Arıca, Biosorption of benzidine based textile dyes Direct Blue 1 and Direct Red 128 using native and heat-treated biomass of *Trametes versicolor*, J. Hazard. Mater. 143 (2007) 135–143.
[9] K. Vijayaraghavan, Y.S. Yun, Biosorption of C.I. Reactive Black 5 from aqueous solution using acid-treated biomass of brown seaweed *Laminaria* sp., Dyes Pigments 76 (2008) 726–732.
[10] T. Akar, İ. Tosun, Z. Kaynak, E. Kavas, G. Incirkus, S.T. Akar, Assessment of the biosorption characteristics of a macro-fungus for the decolorization of Acid Red 44 (AR44) dye, J. Hazard. Mater. 171 (2009) 865–871.
[11] S.T. Akar, A.S. Özcan, T. Akar, A. Özcan, Z. Kaynak, Biosorption of a reactive textile dye from aqueous solutions utilizing an agro-waste, Desalination 249 (2009) 757–761.
[12] F. Çolaka, N. Atarb, A. Olgun, Biosorption of acidic dyes from aqueous solution by *Paenibacillus macerans*: kinetic, thermodynamic and equilibrium studies, Chem. Eng. J. 150 (2009) 122–130.
[13] S.T. Akar, A. Gorgulu, Z. Kaynak, B. Anilan, T. Akar, Biosorption of Reactive Blue 49 dye under batch and continuous mode using a mixed biosorbent of macro-fungus *Agaricus bisporus* and *Thuja orientalis* cones, Chem. Eng. J. 148 (2009) 26–34.
[14] M.C. Ncibi, B. Mahjoub, A.M. Ben Hamissa, R. Ben Mansour, M. Seffen, Biosorption of textile metal-complexed dye from aqueous medium using *Posidonia oceanica* (L.) leaf sheaths: mathematical modeling, Desalination 243 (2009) 109–121.
[15] L.D. Fiorentin, D.E.G. Trigueros, A.N. Módenes, F.R. Espinoza-Quiñones, N.C. Pereira, S.T.D. Barros, O.A.A. Santos, Biosorption of reactive blue 5G dye onto drying orange bagasse in batch system: kinetic and equilibrium modeling, Chem. Eng. J. 163 (2010) 68–77.
[16] Z. Aksu, E. Balibek, Effect of salinity on metal-complex dye biosorption by *Rhizopus arrhizus*, J. Environ. Manage. 91 (2010) 1546–1555.
[17] T.L. Hu, Sorption of reactive dyes by *Aeromonas* biomass, Water Sci. Technol. 26 (1992) 357–366.
[18] L. Velásquez, J. Dussan, Biosorption and bioaccumulation of heavy metals on dead and living biomass of *Bacillus sphaericus*, J. Hazard. Mater. 167 (2009) 713–716.
[19] L.N. Du, Y.Y. Yang, L. Gang, S. Wang, X.M. Jia, Y.H. Zhao, Optimization of heavy metal-containing dye Acid Black 172 decolorization by *Pseudomonas* sp. strain DY1 using statistical designs, Int. Biodeterior. Biodegrad. 64 (2010) 566–573.
[20] T. Akar, I. Tosun, Z. Kaynak, E. Ozkara, O. Yeni, E.N. Sahin, S.T. Akar, An attractive agro-industrial by-product in environmental cleanup: dye biosorption potential of untreated olive pomace, J. Hazard. Mater. 166 (2009) 1217–1225.
[21] K. Vijayaraghavan, J. Mao, Y.S. Yun, Biosorption of methylene blue from aqueous solution using free and polysulfone-immobilized *Corynebacterium glutamicum*: batch and column studies, Bioresour. Technol. 99 (2008) 2864–2871.
[22] L.C. Fang, P. Cai, W.L. Chen, W. Liang, Z.N. Hong, Q.Y. Huang, Impact of cell wall structure on the behavior of bacterial cells in the binding of copper and cadmium, Colloids Surf. A: Physicochem. Eng. Aspects 347 (2009) 50–55.
[23] J.S. Cox, D.S. Smith, L.A. Warren, F.G. Ferris, Characterizing heterogeneous bacterial surface functional groups using discrete affinity spectra for proton binding, Environ. Sci. Technol. 33 (1999) 4514–4521.
[24] E.K. Putra, R. Pranowo, J. Sunarso, N. Indraswati, S. Ismadji, Performance of activated carbon and bentonite for adsorption of amoxicillin from wastewater: mechanisms, isotherms and kinetics, Water Res. 43 (2009) 2419–2430.
[25] S.Garip, A.C. Gozen, F. Severcan, Use of Fourier transform infrared spectroscopy for rapid comparative analysis of *Bacillus* and *Micrococcus* isolates, Food Chem. 113 (2009) 1301–1307.
[26] C.Y. Jia, D.Z. Wei, W.G. Liu, C. Han, S.L. Gao, Y.J. Wang, Selective adsorption of bacteria on sulfide minerals surface, Trans. Nonferrous Met. Soc. China 18 (2008) 1247–1252.
[27] Z. Filip, S. Hermann, An attempt to differentiate *Pseudomonas* spp. and other soil bacteria by FT-IR spectroscopy, Eur. J. Soil Biol. 37 (2001) 137–143.
[28] S.W. Won, M.H. Han, Y.S. Yun, Different binding mechanisms in biosorption of reactive dyes according to their reactivity, Water Res. (2008) 4847–4855.
[29] Y. Zhang, D. Wei, R. Huang, M. Yang, S. Zhang, X. Dou, D. Wang, V. Vimonses, Binding mechanisms and QSAR modeling of aromatic pollutant biosorption on *Penicillium oxalicum* biomass, Chem. Eng. J. 166 (2011) 624–630.
[30] J. Wang, S.Y. He, L.N. Xu, N. Gu, Transmission electron microscopy and atomic force microscopy characterization of nickel deposition on bacterial cells, Chin. Sci. Bull. 52 (2007) 2919–2924.
[31] S.K. Kazya, S.F. D'Souzab, P. Sar, Uranium and thorium sequestration by a *Pseudomonas* sp.: mechanism and chemical characterization, J. Hazard. Mater. 163 (2009) 65–72.
[32] N.S. Maurya, A.K. Mittal, P. Cornel, E. Rother, Biosorption of dyes using dead macro fungi: effect of dye structure, ionic strength and pH, Bioresour. Technol. 97 (2006) 512–521.
[33] A. Srinivasan, T. Viraraghavan, Decolorization of dye wastewaters by biosorbents: a review, J. Environ. Manage. 91 (2010) 1915–1929.